

Bottomonia production in AA collisions

Michael Strickland

Kent State University
Kent, OH USA

Collaborators: B. Krouppa, A. Rothkopf, and R. Ryblewski

12th International Workshop on Heavy Quarkonium

Beijing, China

November 7, 2017



U.S. DEPARTMENT OF
ENERGY

Heavy Quarkonia Suppression

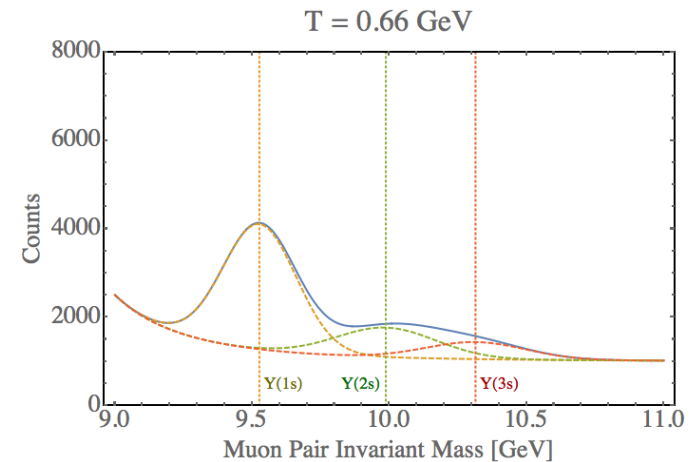
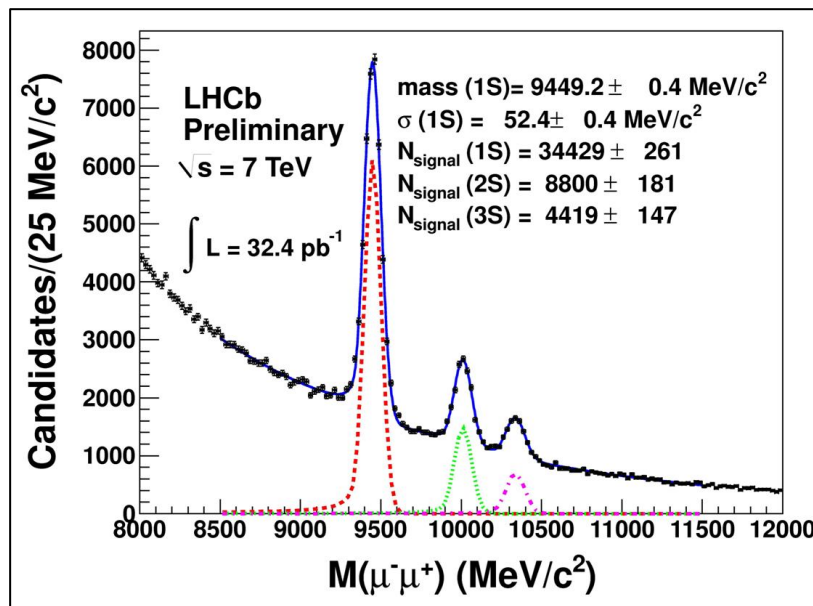
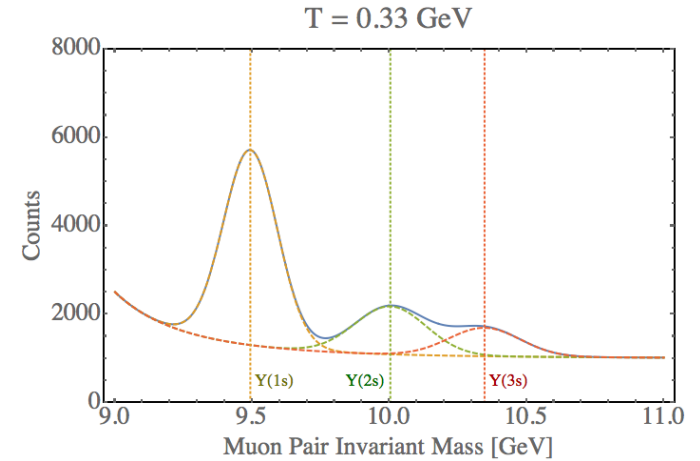
- In a high temperature quark-gluon plasma we expect **weaker color binding** (Debye screening + asymptotic freedom)

E. V. Shuryak, Phys. Rept. 61, 71–158 (1980)

T. Matsui, and H. Satz, Phys. Lett. B178, 416 (1986)

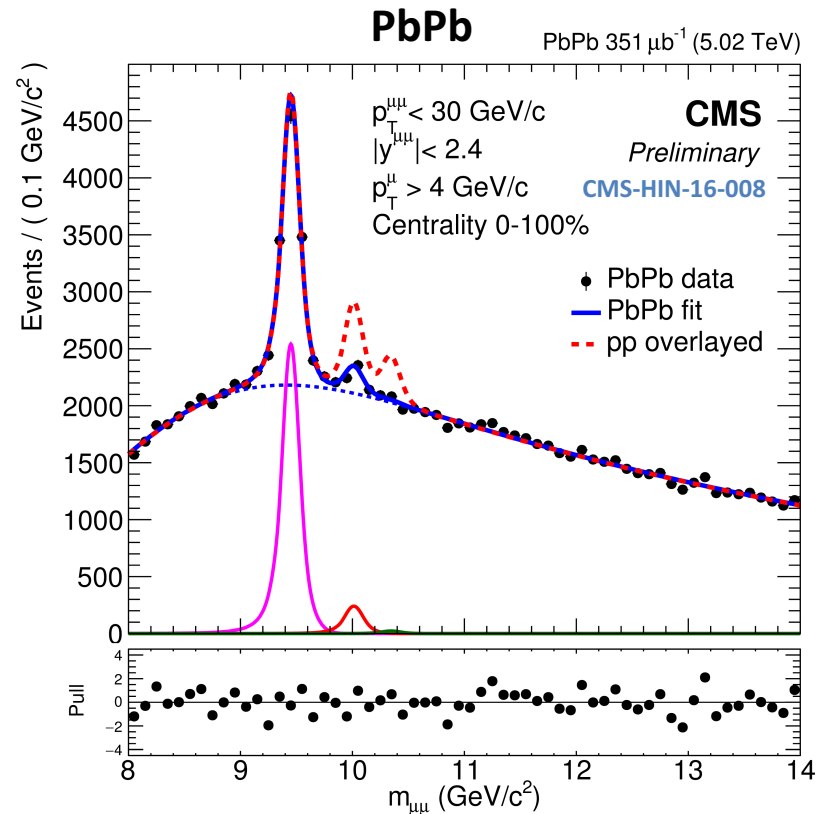
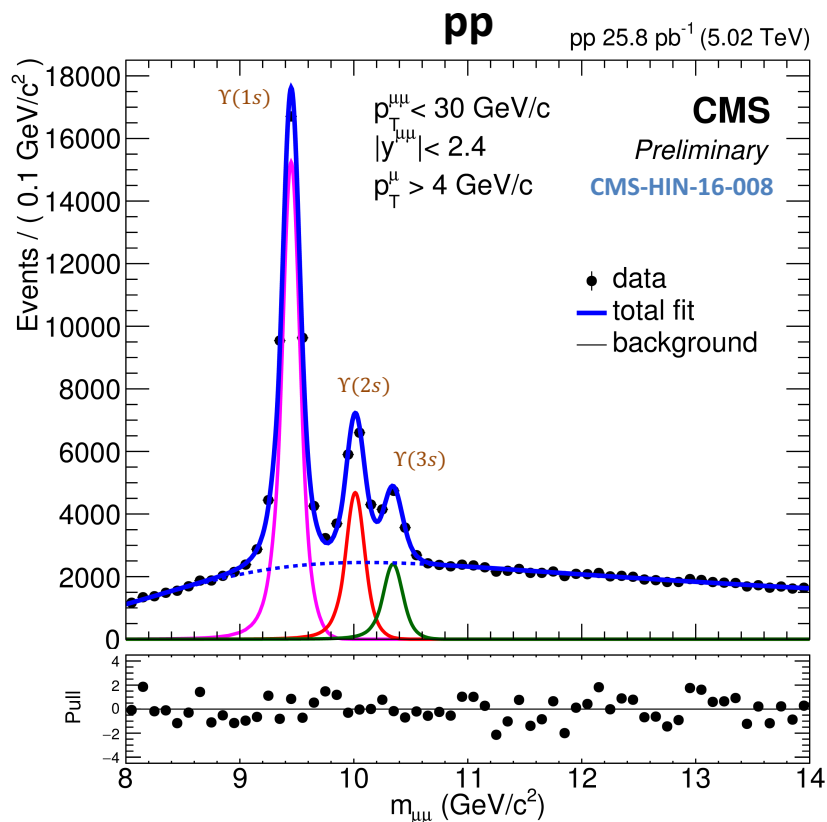
F. Karsch, M. T. Mehr, and H. Satz, Z. Phys. C37, 617 (1988)

- Also, high energy plasma particles which slam into the bound states cause them to have shorter lifetimes → **larger spectral widths**



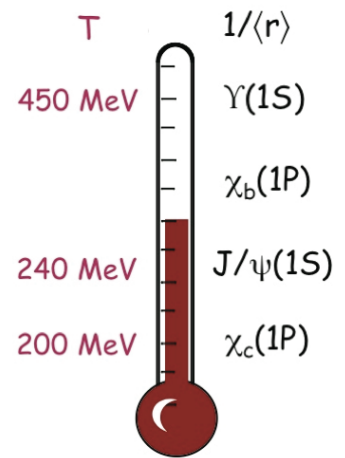
2016 CMS Data – 5.02 TeV Dimuon Spectra

The **CMS** (Compact Muon Solenoid) experiment has measured bottomonium spectra for both pp and Pb-Pb collisions. With this we can extract R_{AA} experimentally.



Why Bottomonia in A-A?

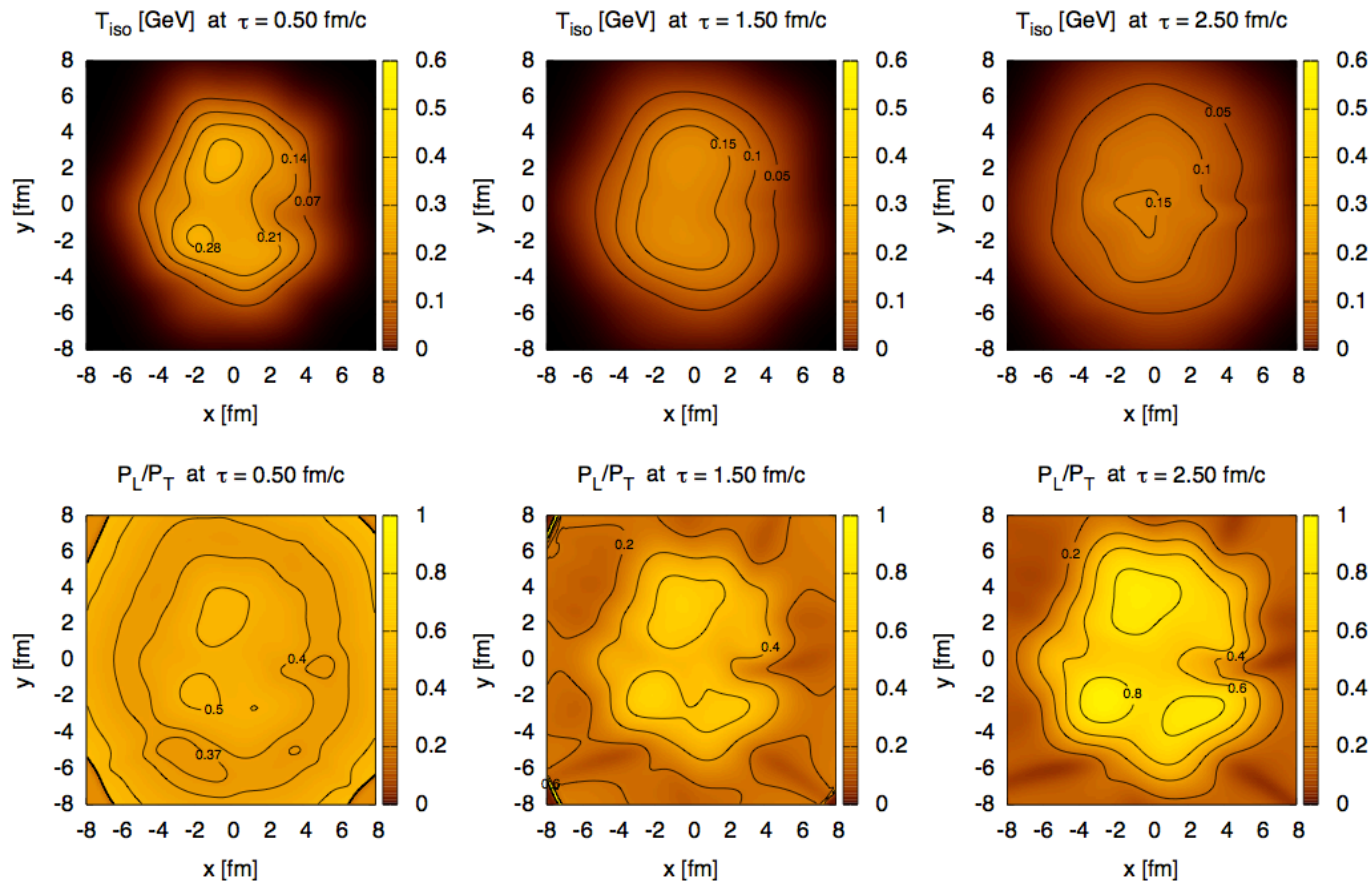
- **Smoking gun for QGP creation**
- Suppression of quarkonia can provide information about the QGP, e.g. initial temperature, etc.
- HQET on surer footing for bottomonia
- Cold nuclear matter (CNM) effects are expected to be much smaller than for the charmonia
- The masses of bottomonia are much higher than the temperature ($T < 1$ GeV) generated in HICs
→ bottomonia production in AA dominated by initial hard scatterings
- Bottom quarks and anti-quarks are relatively rare in LHC HICs → the probability for regeneration of bottomonia through statistical recombination is expected to be less important than for charm quarks [see e.g. E. Emerick, X. Zhao, and R. Rapp, arXiv:1111.6537; Krouppa and MS, forthcoming]



A. Mocsy, P. Petreczky,
and MS, 1302.2180

Conceptually simple calculation

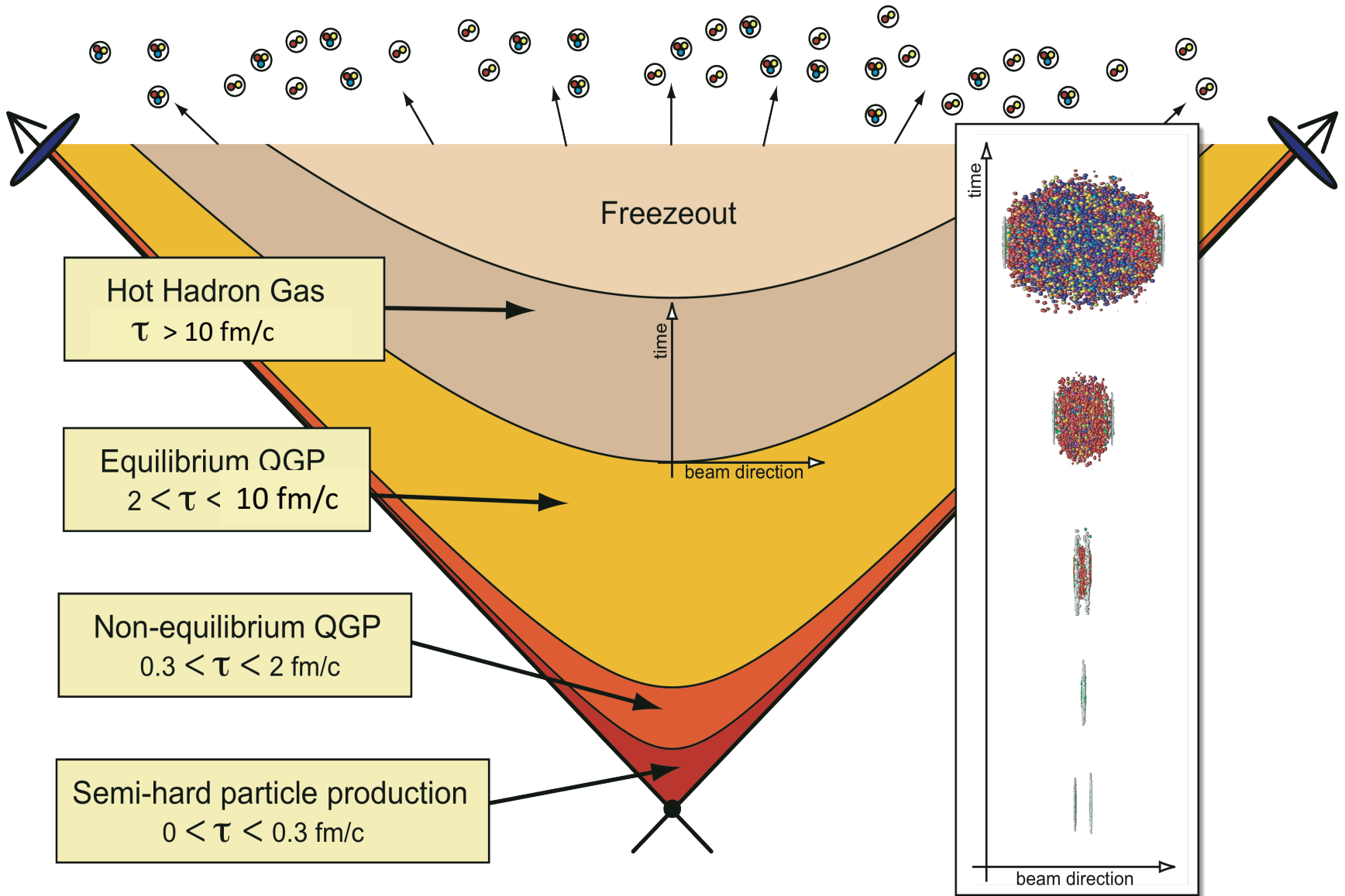
For in-medium suppression, given the population of quarkonia states at some τ_0 , we can simply integrate the instantaneous decay/regeneration rate of the state $\Gamma(\tau, x, y, \eta)$ over the QGP spatiotemporal evolution to obtain the **survival probability**.



Pb-Pb @ 2.76 TeV
 $T_0 = 600$ MeV
 $\tau_0 = 0.25$ fm/c
 $b = 7$ fm

M. Martinez, R. Ryblewski, MS, arXiv:1204.1473

LHC Heavy Ion Collision Timescales



The ingredients

- We use a complex-valued potential.
- The imaginary part of the potential encodes information about the in-medium width.
[Laine et al hep-ph/0611300](#)
- We extended this to include effects of momentum-space anisotropy (non-eq correction).
[Dumitru, Guo, and MS, 0711.4722 and 0903.4703; see also Burnier, Laine, Vepsalainen, arXiv:0903.3467](#)
- From this, we obtain the real and imaginary parts of the binding energy.
- These are then folded together with the full 3+1d dynamical QGP evolution provided by dissipative anisotropic hydrodynamics.
- In all of our published results, we have not included CNM or regeneration. At the end of my talk, I will present our first preliminary results including regeneration.

Summary of the method

Solve the 3d Schrödinger EQ
with complex-valued potential

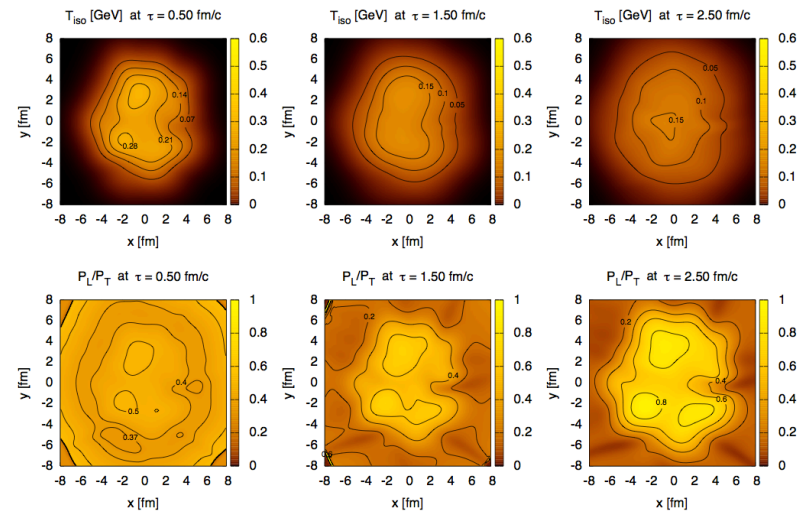
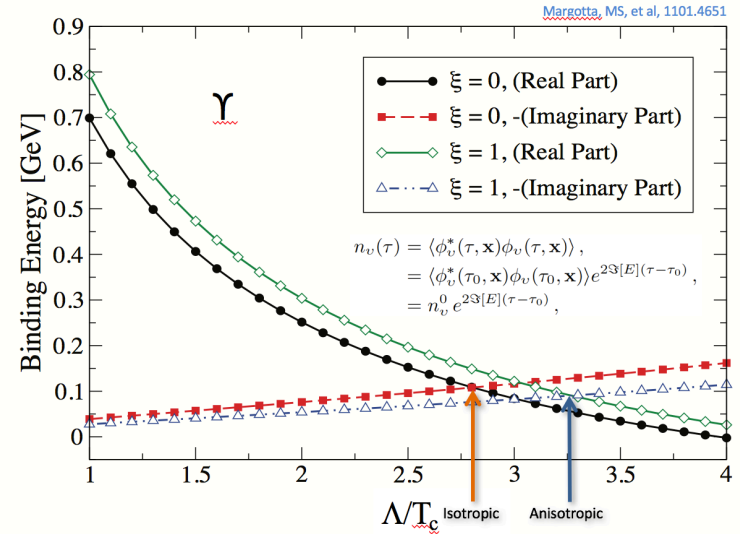


Obtain real and imaginary parts of
the binding energies for the $\Upsilon(1s)$,
 $\Upsilon(2s)$, $\Upsilon(3s)$, χ_{b1} , and χ_{b2} as function
of energy density and anisotropy.

Yager-Elorriaga and MS, 0901.1998; Margotta, MS, et al,
1101.4651

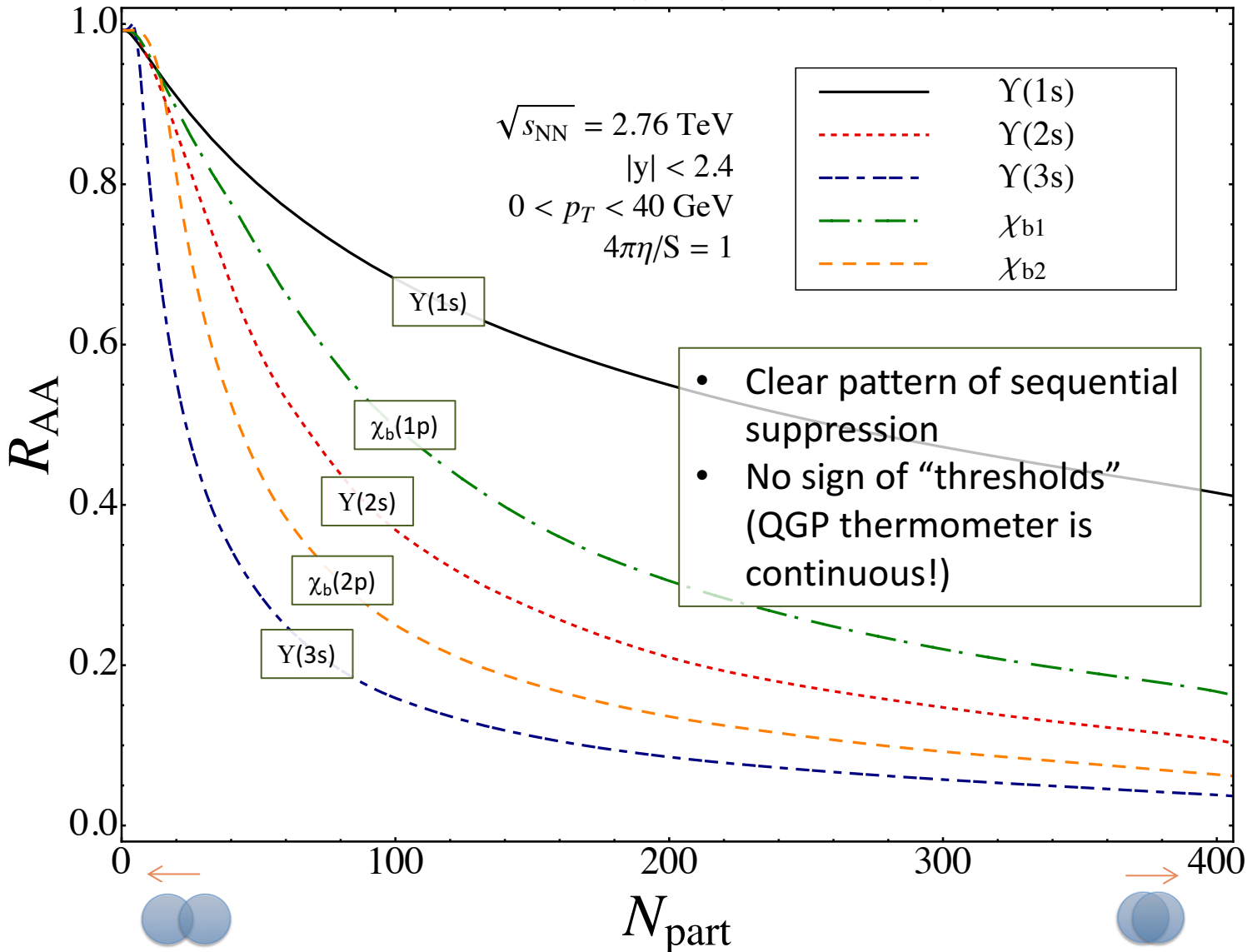


Fold together with the non-EQ
spatiotemporal evolution to
obtain the **survival probability**.



State Suppression Factors, R_{AA}^i

B. Krouppa, R. Ryblewski, and MS, Phys. Rev. C 92, 061901(R)(2015).



Y(1S) Feed Down Fractions

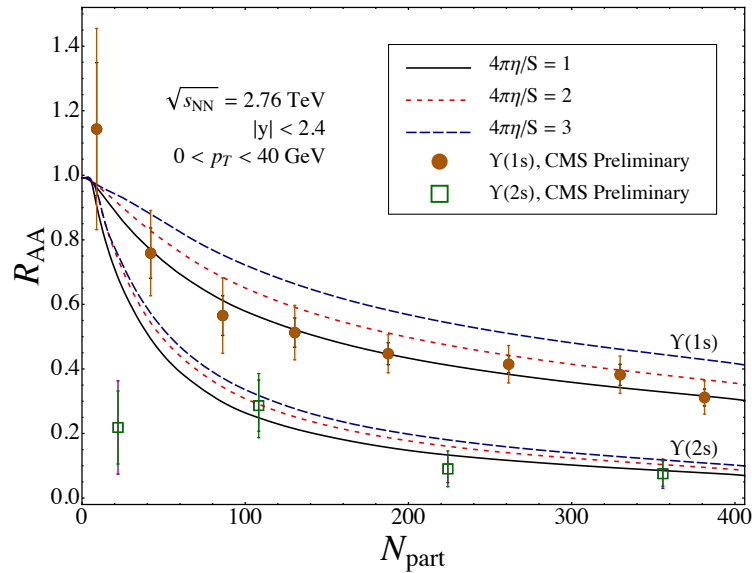
Y(1S)	0.668
Y(2S)	0.086
Y(3S)	0.010
$\chi_{b(1P)}$	0.170
$\chi_{b(2P)}$	0.051
$\chi_{b(3P)}$	0.015

Y(2S) Feed Down Fractions

Y(2S)	0.604
Y(3S)	0.043
$\chi_{b(2P)}$	0.309
$\chi_{b(3P)}$	0.044

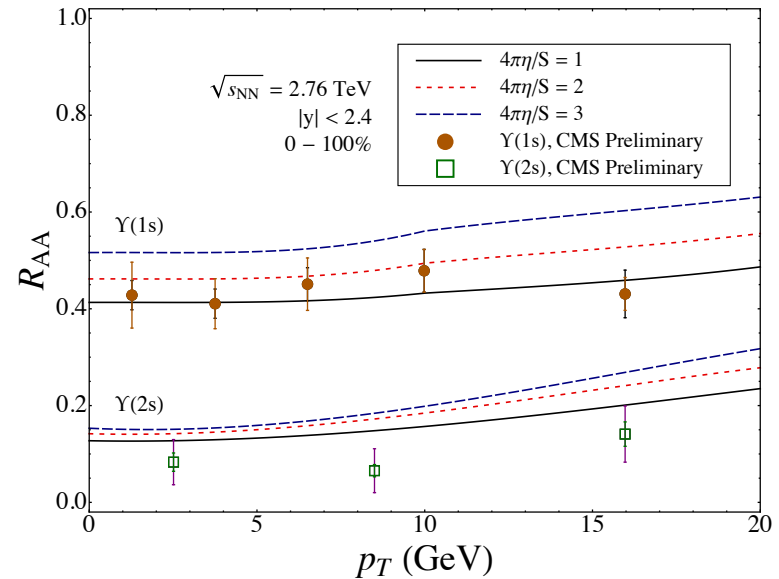
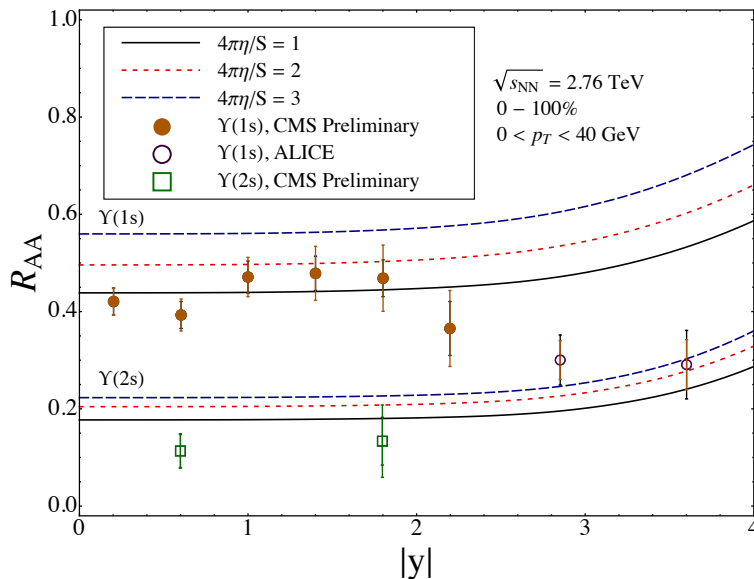
Inclusive Bottomonium Suppression @ 2.76 TeV

B. Krouppa, R. Ryblewski, and MS, Phys. Rev. C 92, 061901(R) (2015).



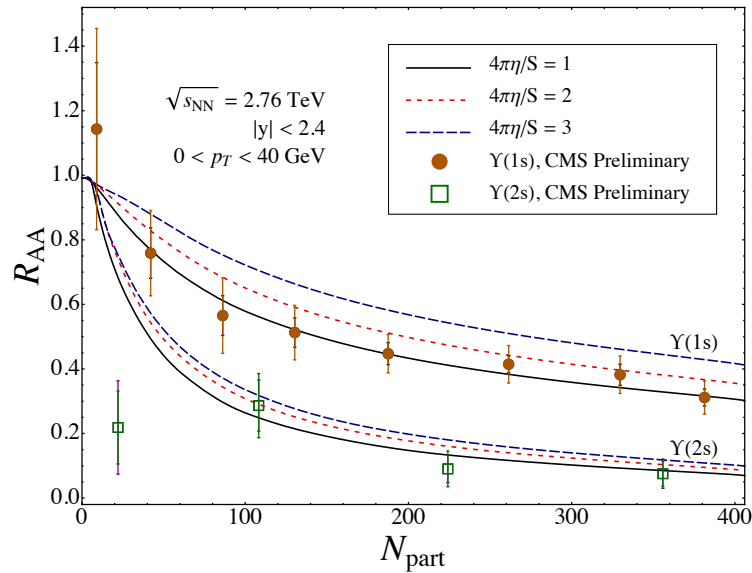
- Compare model to 2.76 TeV data from CMS and ALICE
- Reasonable agreement with CMS data but not perfect
- Disagreement with ALICE data in rapidity range $2.5 < y < 4$
- Model under predicts $\Upsilon(2s)$ suppression

$4\pi\eta/s$	T_0 [GeV]
1	0.552
2	0.546
3	0.544

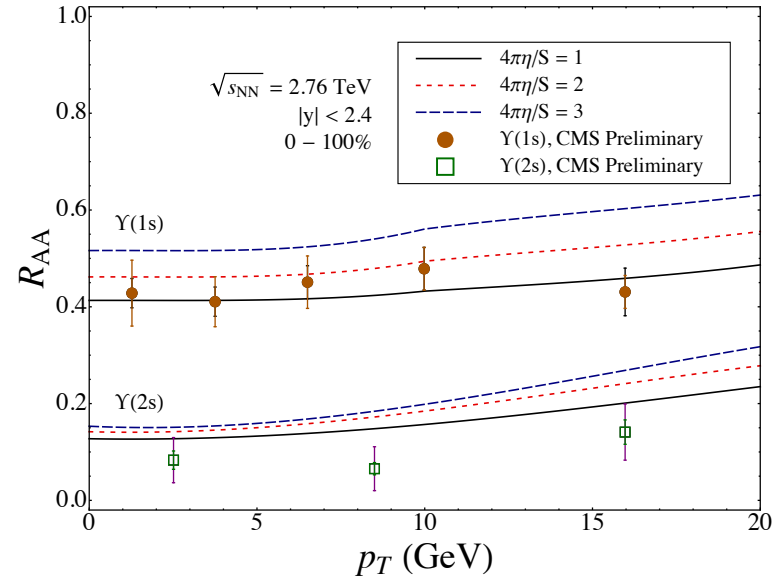
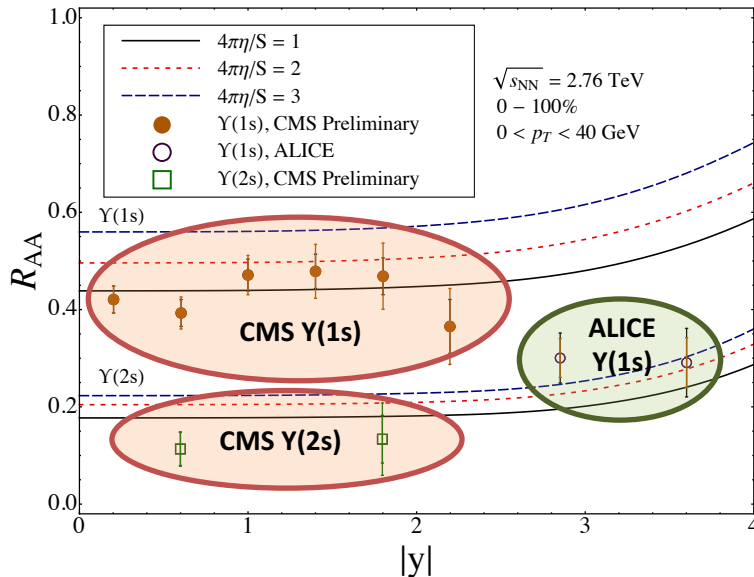


Inclusive Bottomonium Suppression @ 2.76 TeV

B. Krouppa, R. Ryblewski, and MS, Phys. Rev. C 92, 061901(R) (2015).



- Compare model to 2.76 TeV data from CMS and ALICE
- Reasonable agreement with CMS data but not perfect
- Disagreement with ALICE data in rapidity range $2.5 < y < 4$
- Model under predicts $\Upsilon(2s)$ suppression

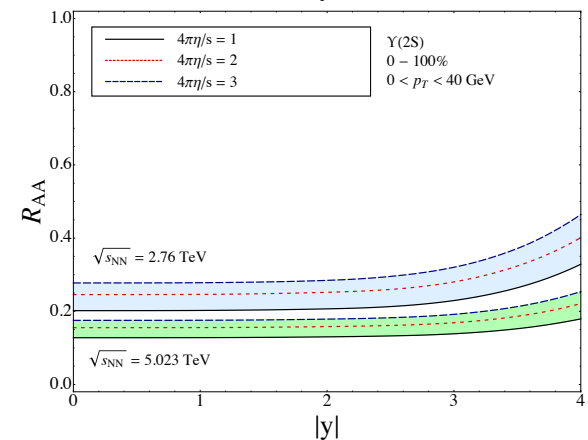
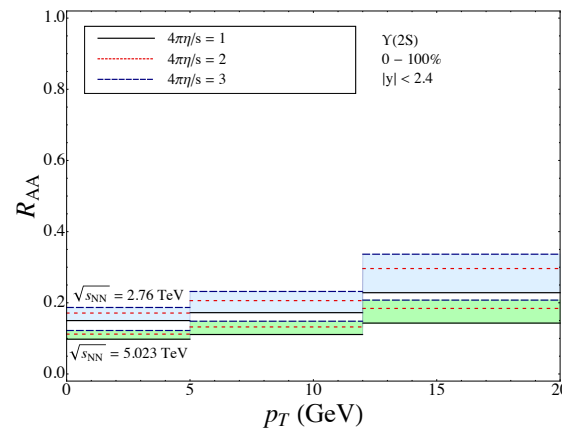
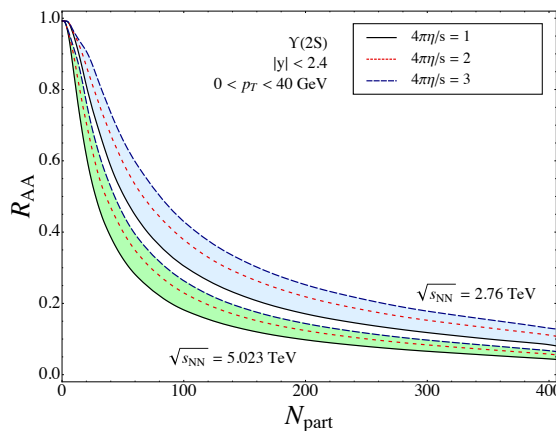
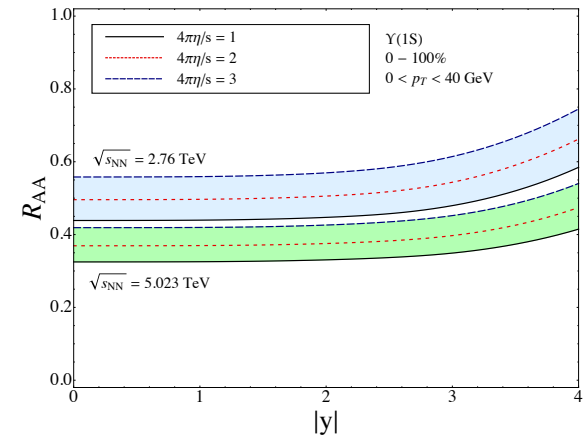
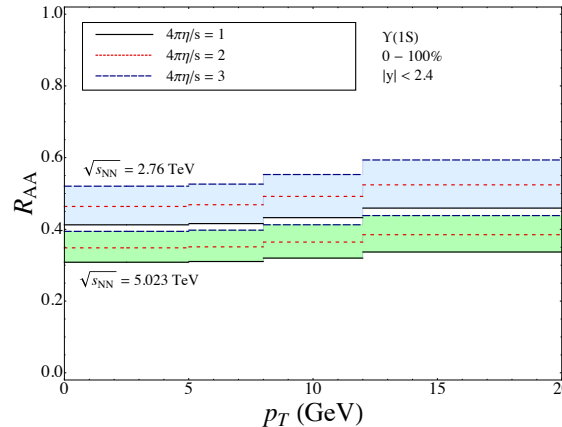
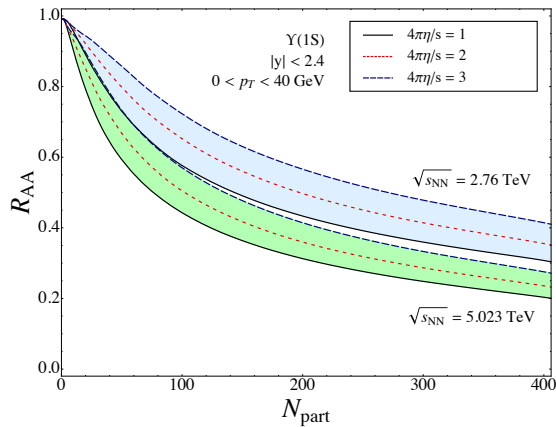


Inclusive Bottomonium Suppression @ 5.02 TeV

B. Krouppa, and MS, Universe 2016, 2(3), 16 (2016).

- We made predictions for 5.02 TeV in May 2016, then nervously waited for the data to appear...

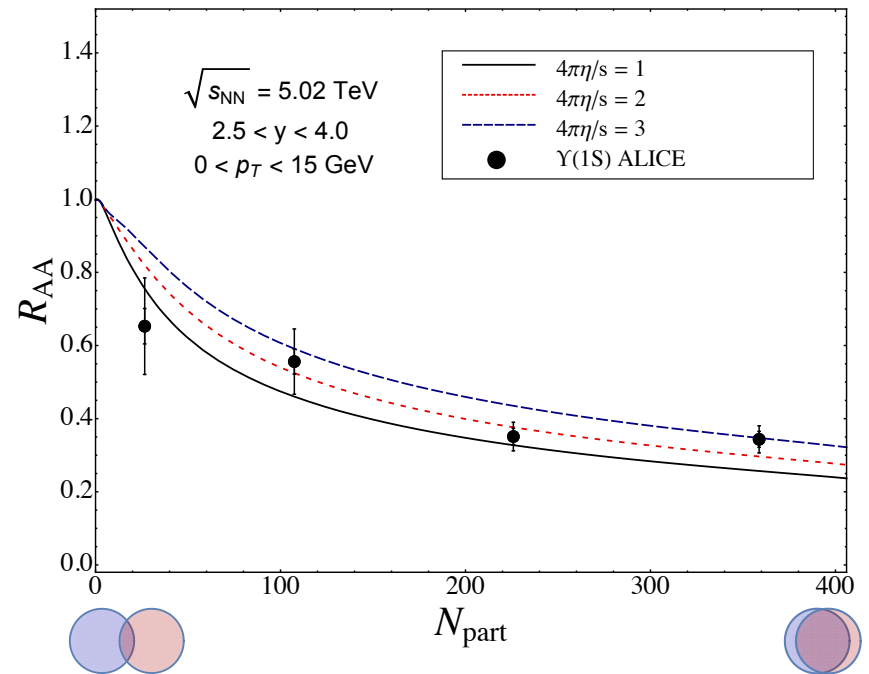
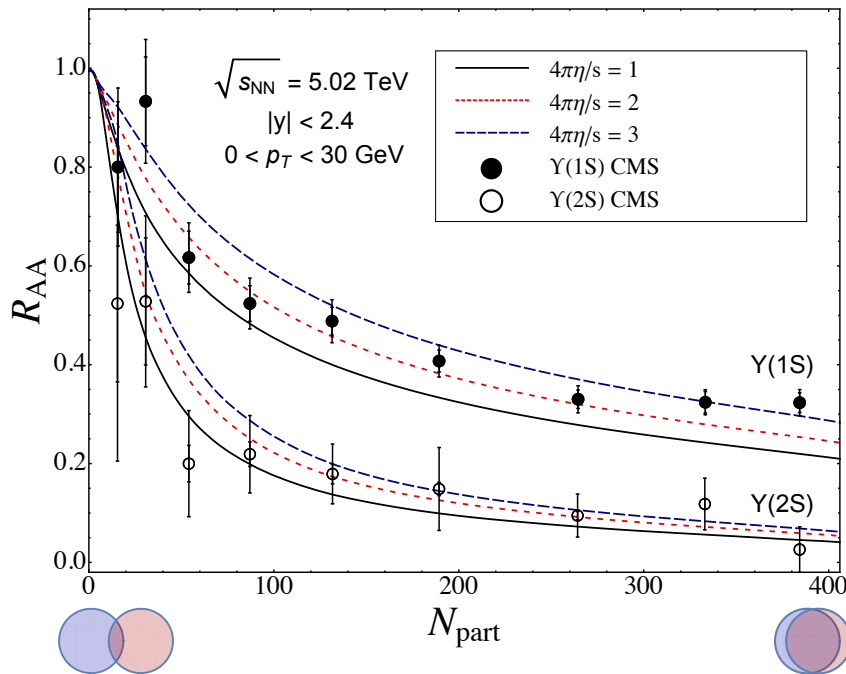
$4\pi\eta/s$	T_0 [GeV]
1	0.641
2	0.632
3	0.629



Inclusive Bottomonium Suppression @ 5.02 TeV

B. Krouppa, R. Ryblewski, and MS 1704.02361

- Model predictions compared to CMS data (left) and ALICE data (right)
- Results below are as a function of N_{part}

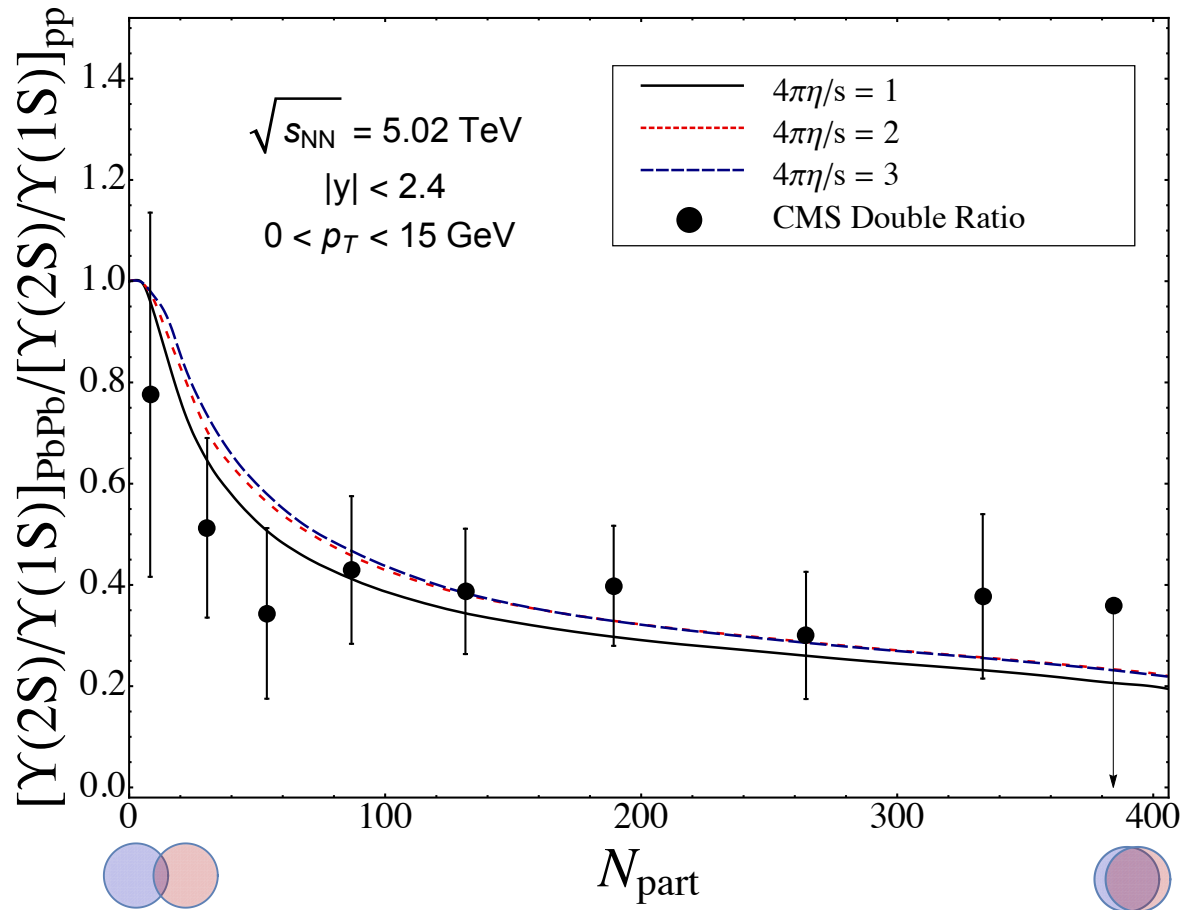


- CMS (left) covers central rapidity ($|y| < 2.4$) and ALICE (right) covers forward rapidity ($2.5 < |y| < 4$)

Inclusive Bottomonium Suppression @ 5.02 TeV

B. Krouppa, R. Ryblewski, and MS 1704.02361

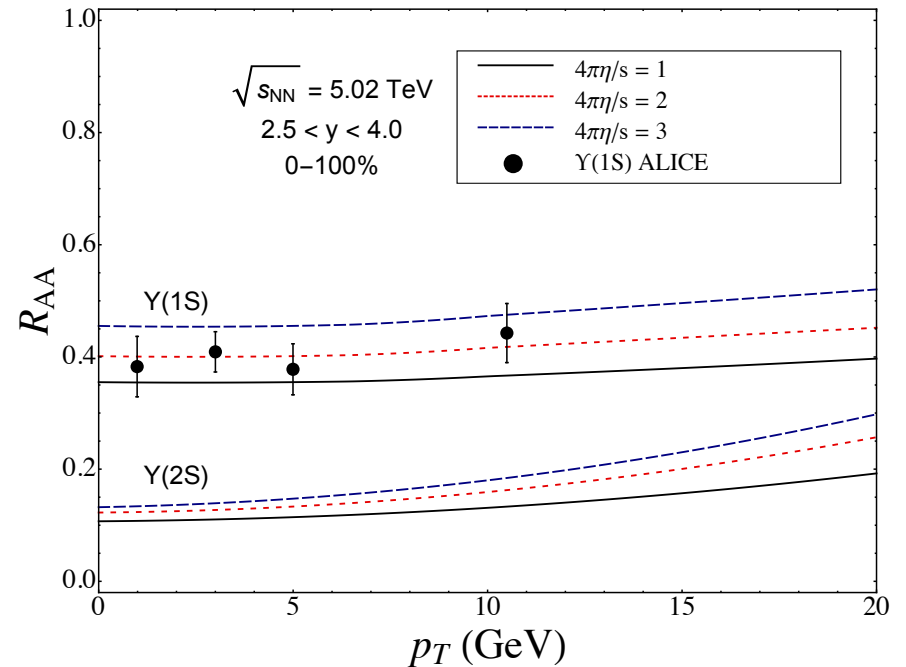
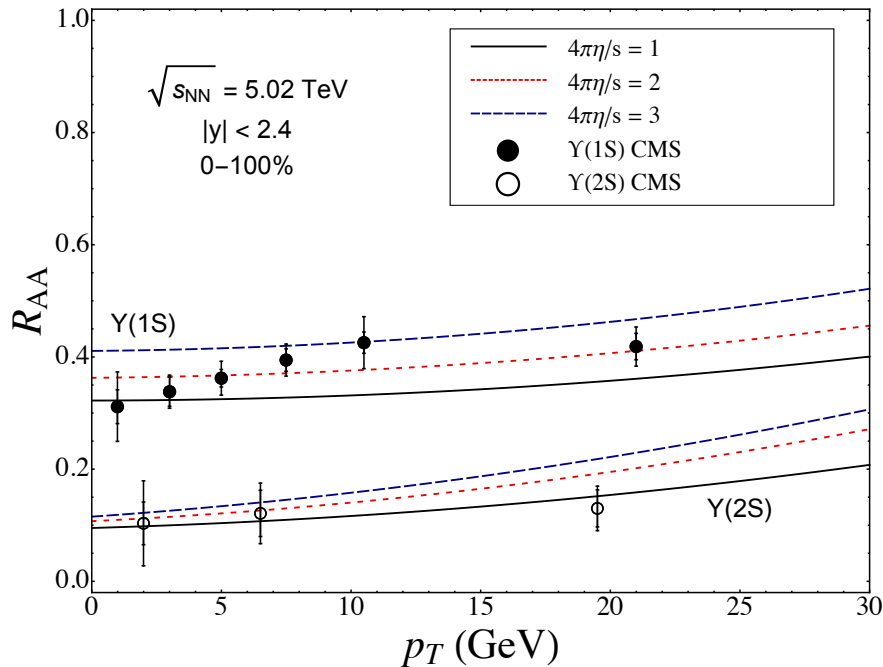
- Model predictions compared to CMS data for the double ratio
- Results below are as a function of N_{part}



Inclusive Bottomonium Suppression @ 5.02 TeV

B. Krouppa, R. Ryblewski, and MS 1704.02361

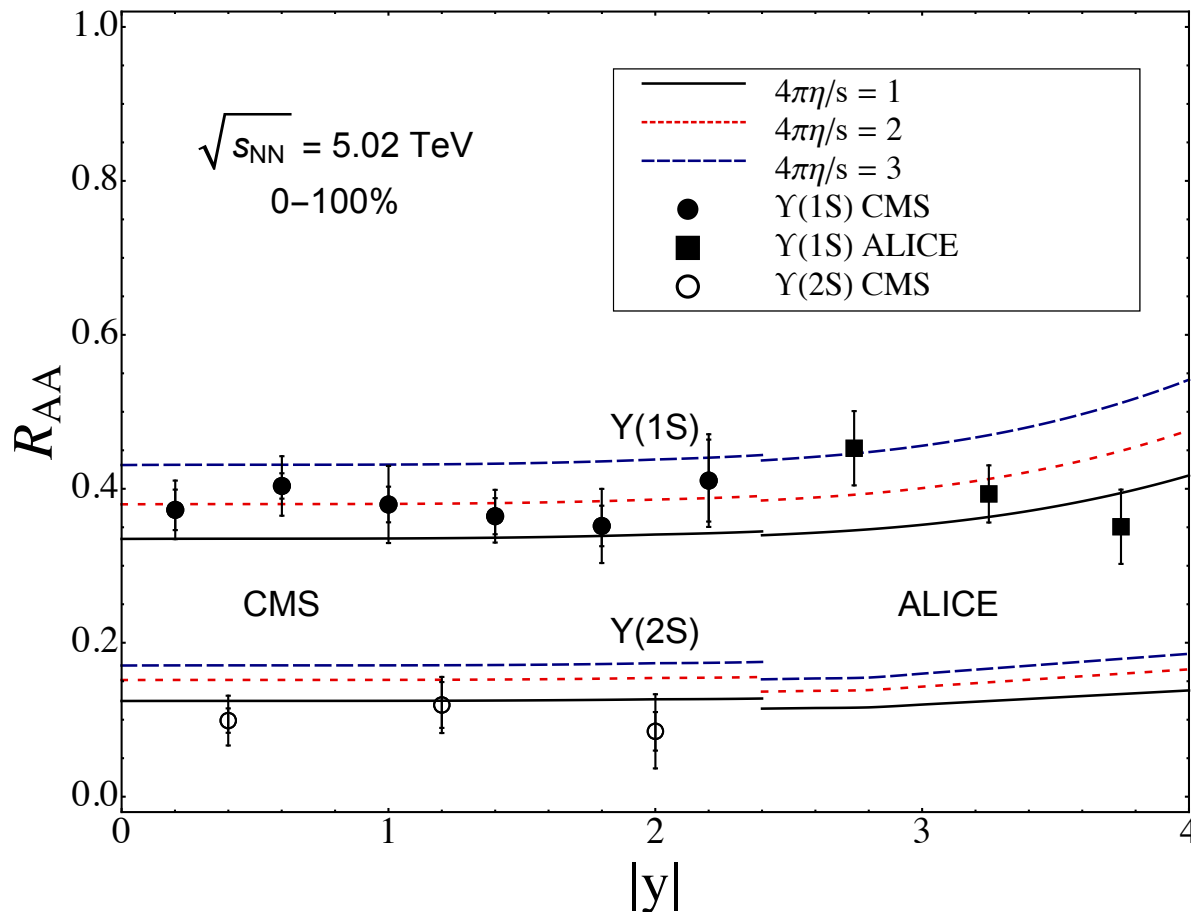
- Model predictions vs CMS data (left) and ALICE data (right);
- Results below are as a function of transverse momentum p_T



Inclusive Bottomonium Suppression @ 5.02 TeV

B. Krouppa, R. Ryblewski, and MS 1704.02361

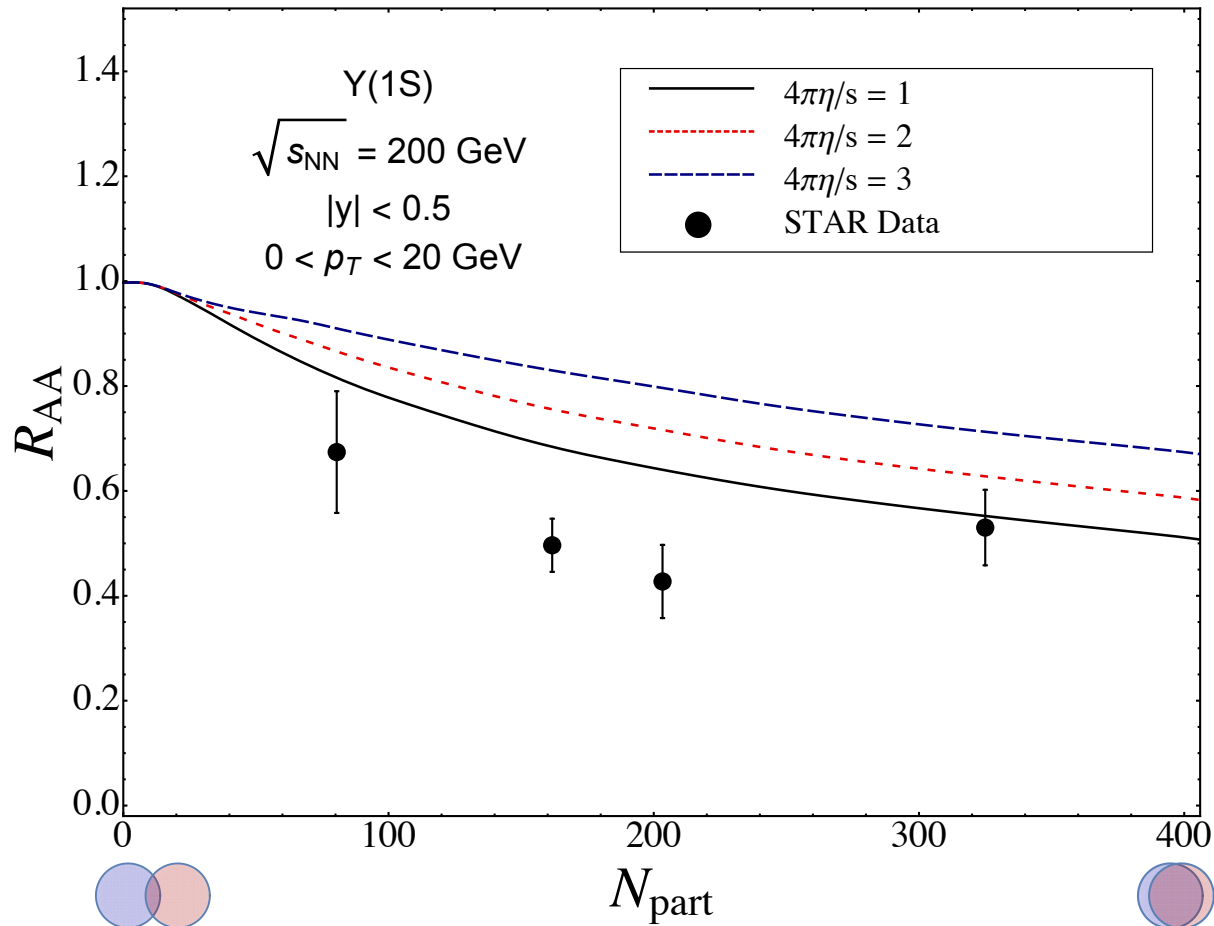
- Model predictions vs CMS and ALICE data (combined in one figure)



Inclusive Bottomonium Suppression @ 200 GeV

B. Krouppa, R. Ryblewski, and MS 1704.02361

- Model predictions compared to recent STAR data



Improving the model

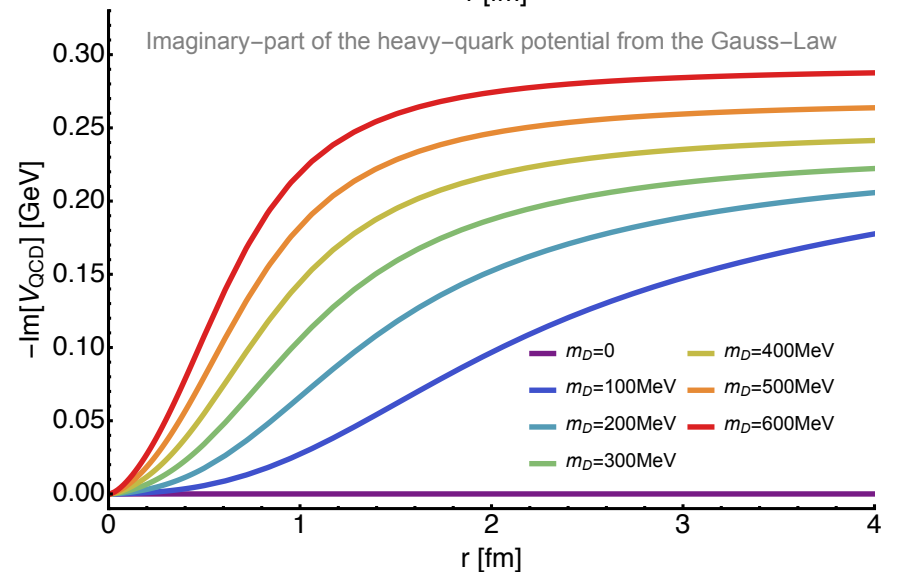
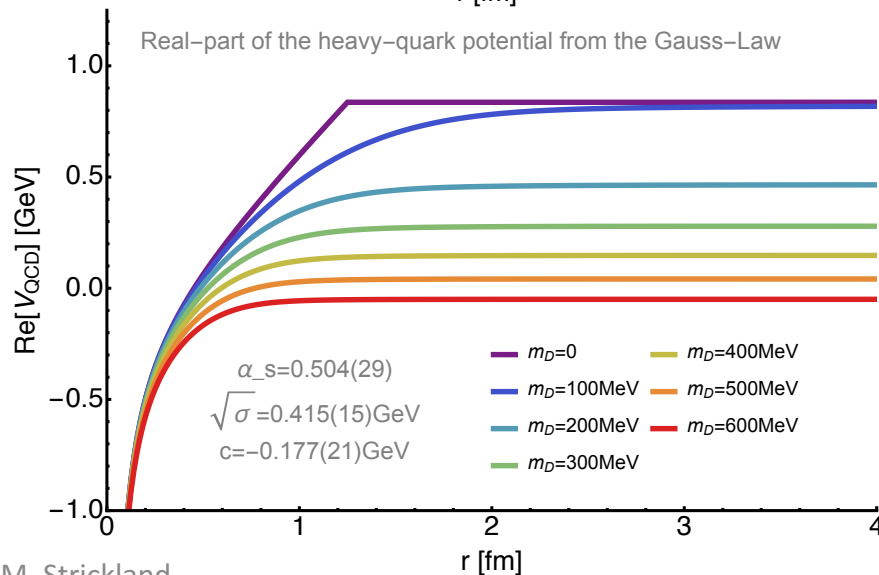
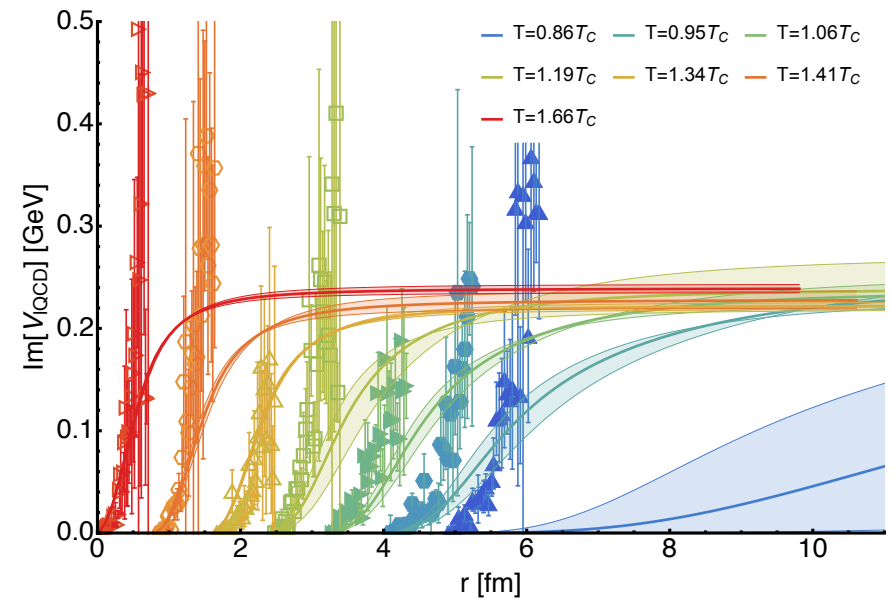
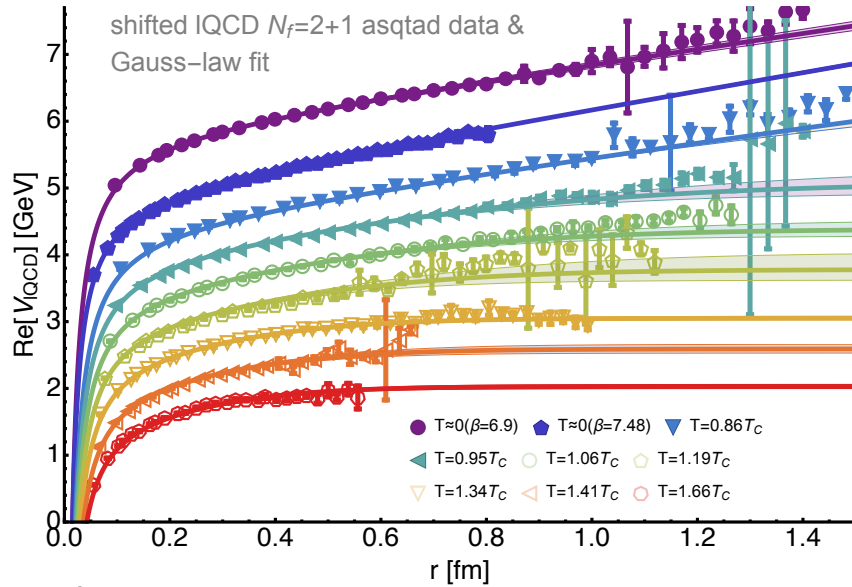
We would like to:

- 1) Constrain/improve the complex-valued potential using finite-T lattice calculations
- 2) Include effects of in-medium regeneration
- 3) Include CNM effects

Today I will report on progress towards goals 1) and 2); Goal 3) will remain on the to-do list for now...

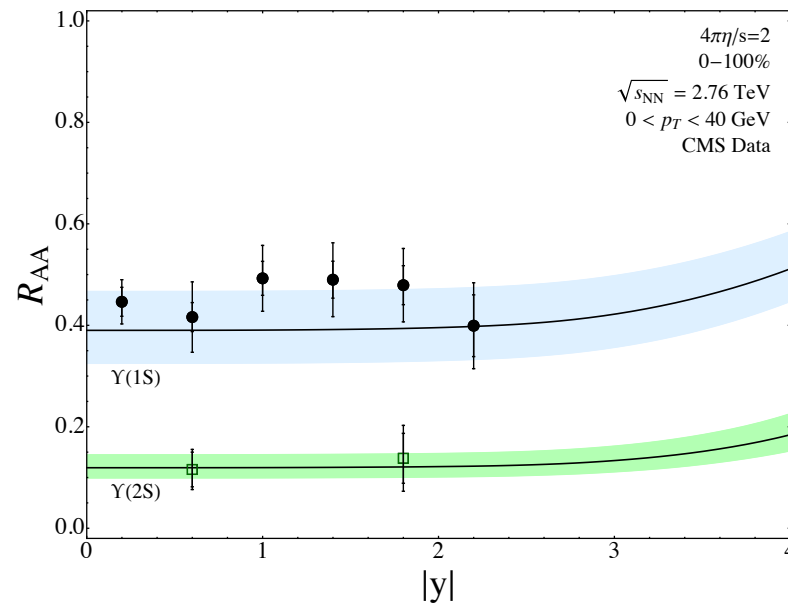
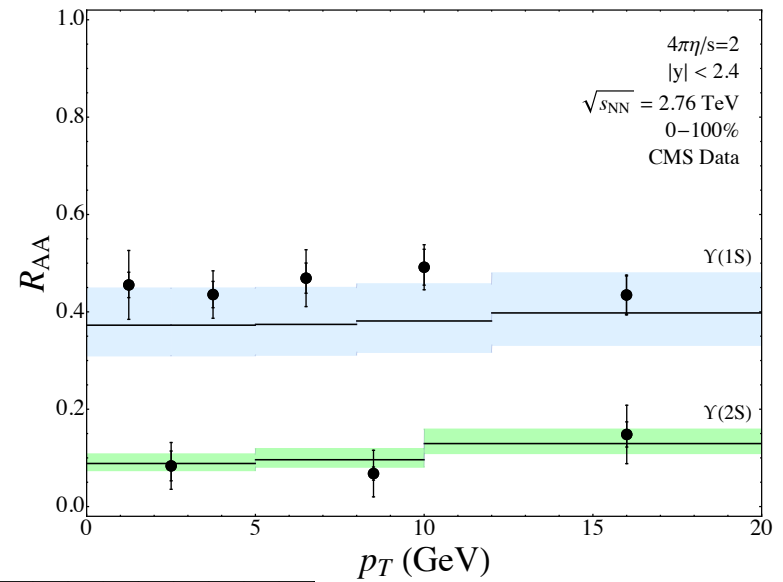
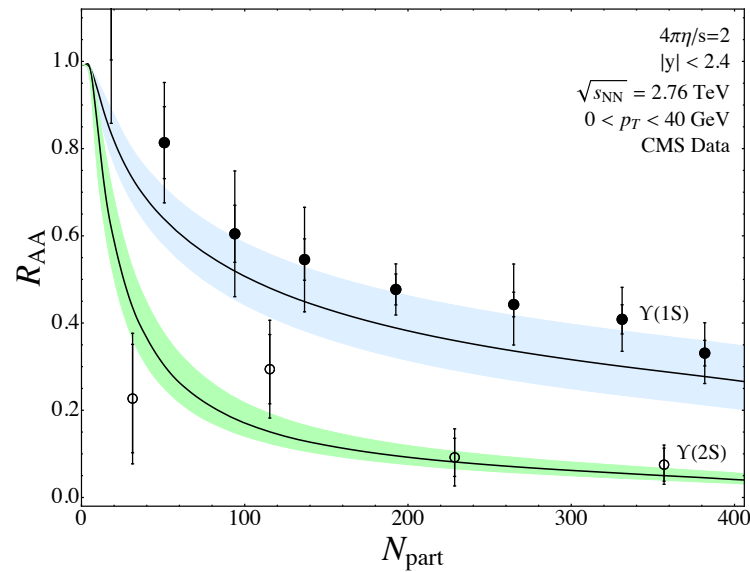
Lattice-vetted potential

B. Kroupa, R. Rothkopf, and MS 1710.02319



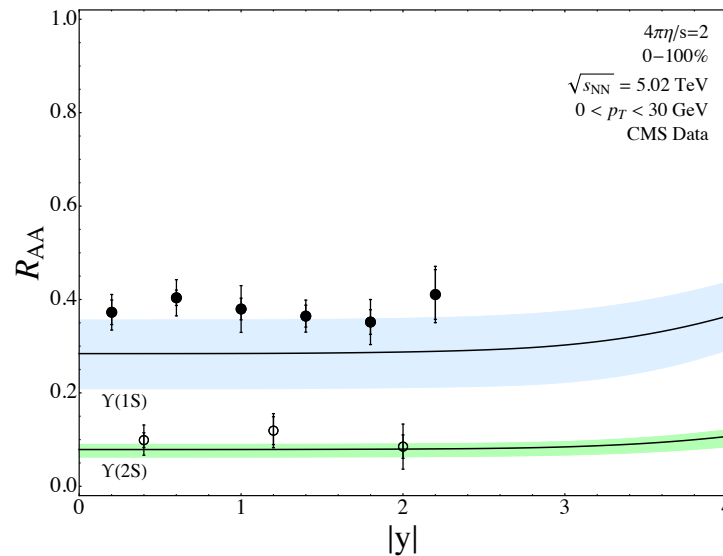
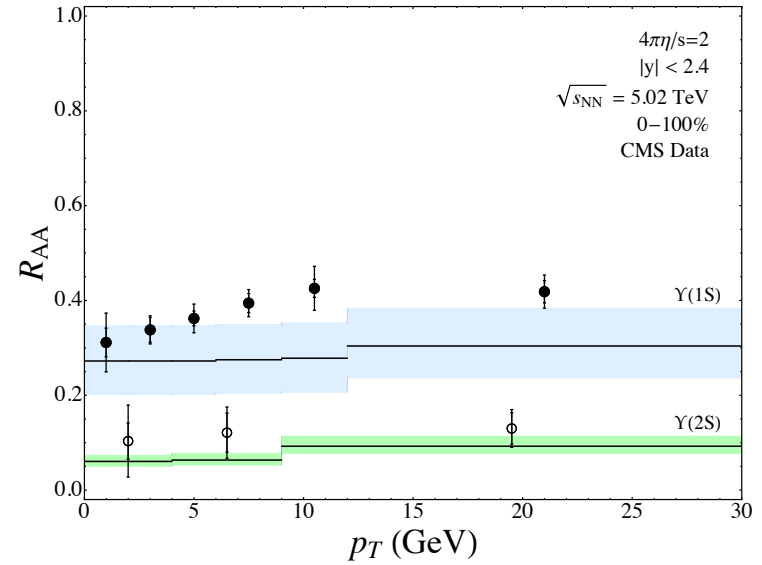
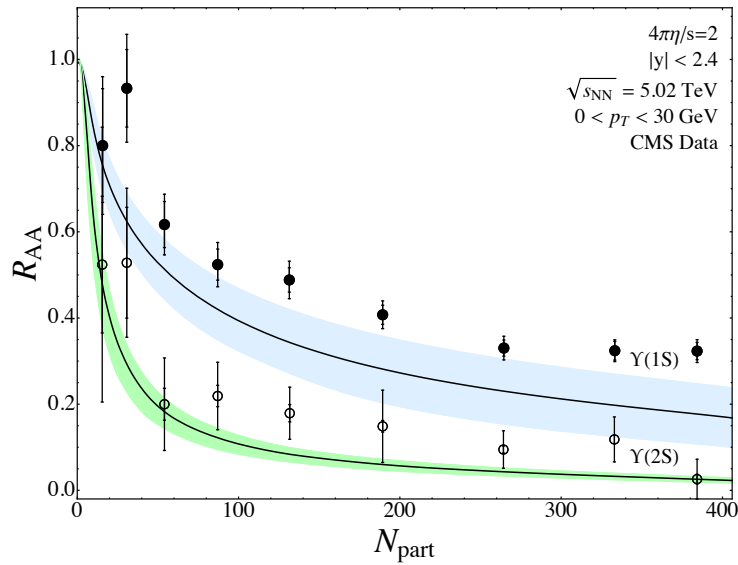
Lattice-vetted potential (2.76 TeV)

B. Krouppa, R. Rothkopf, and MS 1710.02319



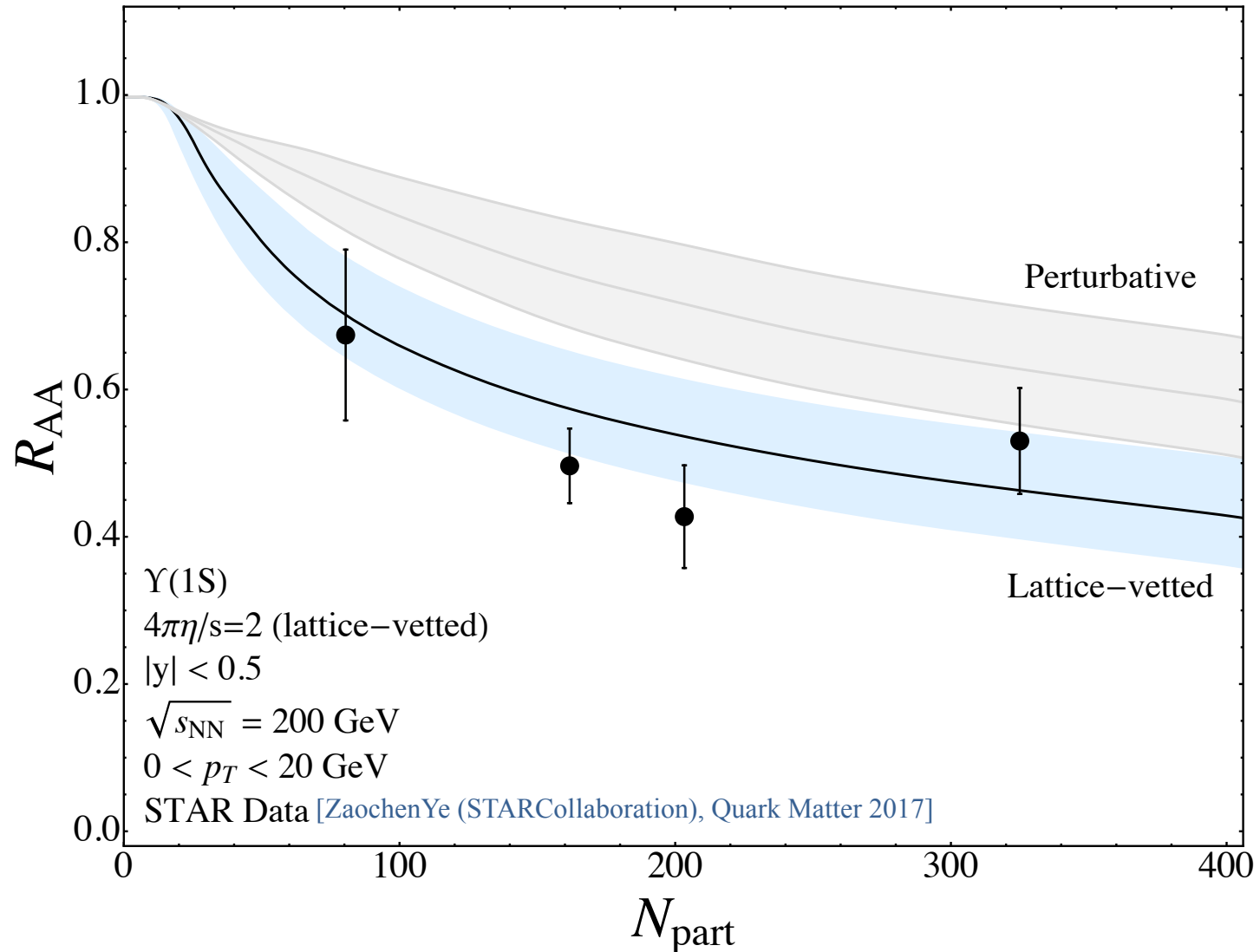
Lattice-vetted potential (5.02 TeV)

B. Krouppa, R. Rothkopf, and MS 1710.02319



Lattice-vetted potential (200 GeV)

B. Krouppa, R. Rothkopf, and MS 1710.02319



Including regeneration

- Solve the Boltzmann equation in 3+1d taking into account the local effective temperature and momentum-space anisotropy.

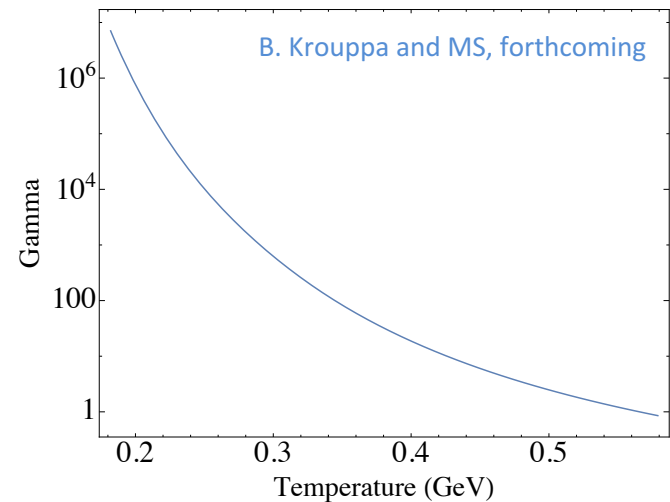
$$\partial_\tau f_\Upsilon(p, x) = -\Gamma(T, \xi) [f_\Upsilon(p, x) - f_{\Upsilon,eq}(p, x)]$$

- Assuming chemical equilibrium between all available bottom-quark states, the $b\bar{b}$ number is matched to the equilibrium numbers of bottom states the fugacity γ_b

$$N_{b\bar{b}} = \frac{1}{2} N_{\text{open}} \frac{I_1(N_{\text{open}})}{I_0(N_{\text{open}})} + N_{\text{hidden}}$$

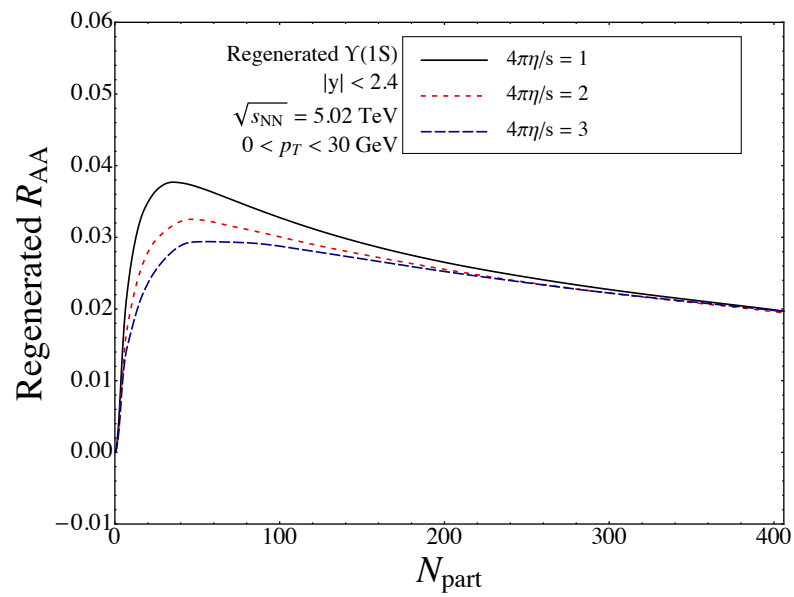
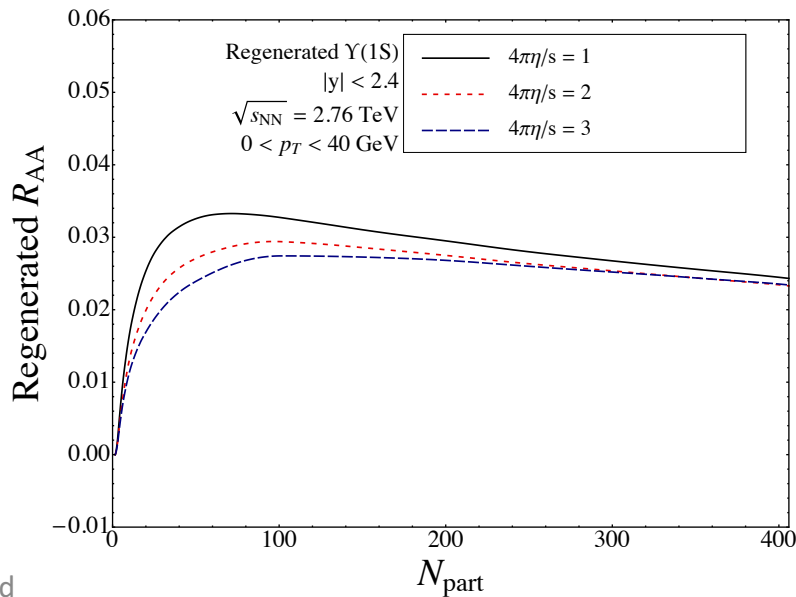
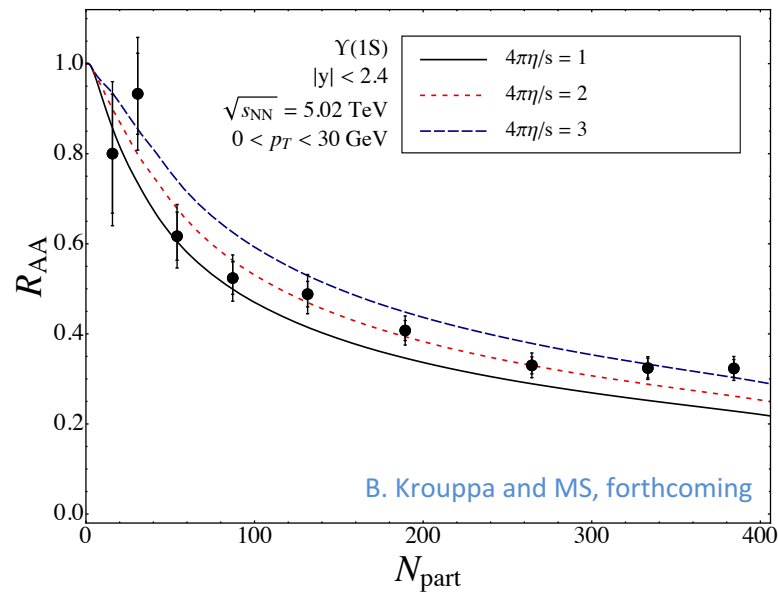
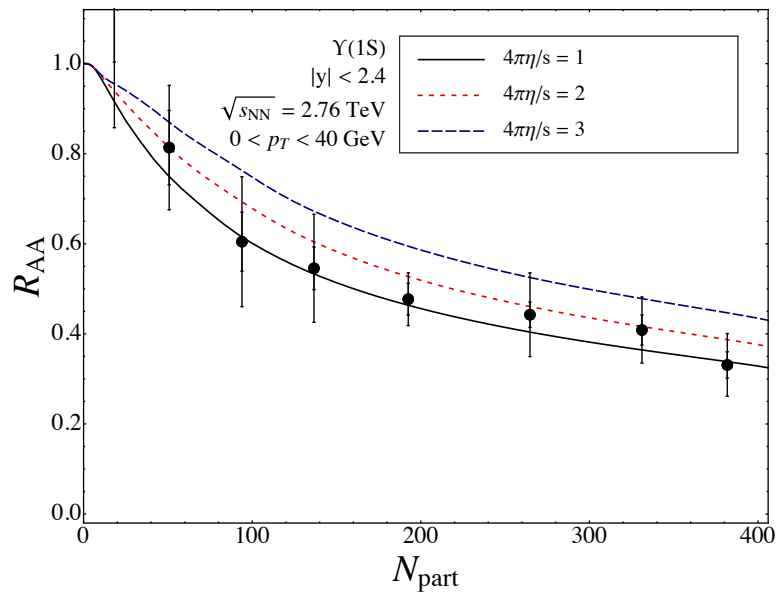
$$N_{\text{open}} = \gamma_b d_b \int_{\mathbf{p}, \mathbf{x}} f_{b,eq}(p, x)$$

$$N_{\text{hidden}} = \gamma_b^2 \sum_{\Upsilon_i} d_i \int_{\mathbf{p}, \mathbf{x}} f_{\Upsilon_i,eq}(p, x)$$



Results (Strickland/Bazow potential)

Preliminary



Conclusions and Outlook

- Complex screening model works reasonably well to describe the suppression seen at LHC for central rapidities. Very good agreement with CMS results at 2.76 and 5.02 TeV.
- Smoking gun for creation of the QGP. Not possible to explain this with pure CNM.
- At forward rapidities, the model is in disagreement with ALICE 2.76 TeV results, however, the 5.02 TeV data from ALICE seem to be consistent with the model predictions
- STAR results for $Y(1s)$ is not well-explained using the model potential, however, our improved lattice-vetted potential does a better job with it. The price is that we break agreement at higher energies.
- Finally, I presented preliminary results of including locally self-consistent dynamical regeneration.

Backup slides

Other pieces of the puzzle

pp reference

Experimental measurements rely on R_{AA} which is **defined relative to the pp cross section**; therefore, we need reliable pp reference data and a firm theoretical understanding of open- and closed-charm production in pp collisions

Cold nuclear matter effects

Quarkonia production is also affected by **nuclear-modified PDFs, Cronin effect, and co-movers** which can result in enhancement or suppression of quarkonia production depending on the kinematic window.

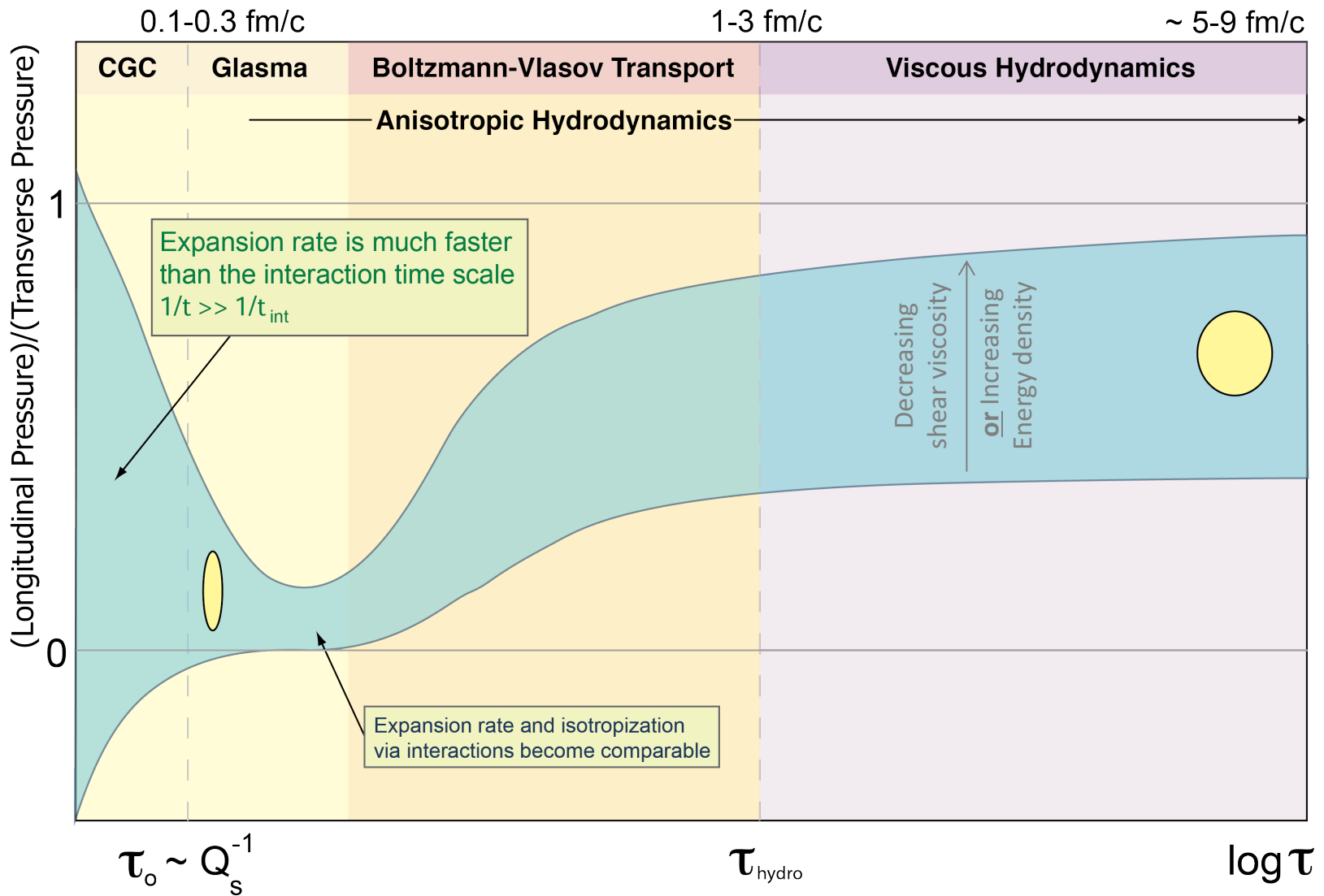
Regeneration

If the population of open- and closed-charm states is high, then it is possible for quarkonia to be regenerated through **recombination of open heavy flavor with a liberated heavy flavor**. There can also be local recombination of an individual bound state due to medium interactions.

Viscous QGP modeling

Quarkonia are sensitive to the full spatio-temporal evolution of the QGP. Need to compute dynamical processes including non-equilibrium corrections. **Should use codes that reproduce experimental data for bulk observables** such as particle spectra and azimuthal flow.

QGP momentum anisotropy cartoon



In-medium heavy quark potential

Using the real-time formalism one can express the potential in terms of the *static* advanced, retarded, and Feynman propagators

$$V(\mathbf{r}, \xi) = -g^2 C_F \int \frac{d^3 \mathbf{p}}{(2\pi)^3} (e^{i\mathbf{p}\cdot\mathbf{r}} - 1) \frac{1}{2} \left(D^{*L}_R + D^{*L}_A + D^{*L}_F \right)$$

Real part can be written as

$$\text{Re}[V(\mathbf{r}, \xi)] = -g^2 C_F \int \frac{d^3 \mathbf{p}}{(2\pi)^3} e^{i\mathbf{p}\cdot\mathbf{r}} \frac{\mathbf{p}^2 + m_\alpha^2 + m_\gamma^2}{(\mathbf{p}^2 + m_\alpha^2 + m_\gamma^2)(\mathbf{p}^2 + m_\beta^2) - m_\delta^4}$$

With direction-dependent masses, e.g.

$$m_\alpha^2 = -\frac{m_D^2}{2p_\perp^2 \sqrt{\xi}} \left(p_z^2 \arctan \sqrt{\xi} - \frac{p_z \mathbf{p}^2}{\sqrt{\mathbf{p}^2 + \xi p_\perp^2}} \arctan \frac{\sqrt{\xi} p_z}{\sqrt{\mathbf{p}^2 + \xi p_\perp^2}} \right)$$

Anisotropic potential calculation: Dumitru, Guo, and MS, 0711.4722 and 0903.4703
 Gluon propagator in an anisotropic plasma: Romatschke and MS, hep-ph/0304092

Complex-valued Potential

- Anisotropic potential can be parameterized as a Debye-screened potential with a direction-dependent Debye mass

$$V_{\text{screened}}(r, \theta, \xi, \Lambda) = -C_F \alpha_s \frac{e^{-\mu(\theta, \xi, \Lambda)r}}{r}$$

[MS, 1106.2571](#); [Bazow and MS, 1112.2761](#)

- The potential also has an imaginary part coming from the Landau damping of the exchanged gluon!

$$V_{\text{R}}(\mathbf{r}) = -\frac{\alpha}{r} (1 + \mu r) \exp(-\mu r) + \frac{2\sigma}{\mu} [1 - \exp(-\mu r)] - \sigma r \exp(-\mu r) - \frac{0.8 \sigma}{m_Q^2 r}$$

Internal Energy

[Dumitru, Guo, Mocsy, and MS, 0901.1998](#)

- This imaginary part also exists in the isotropic case

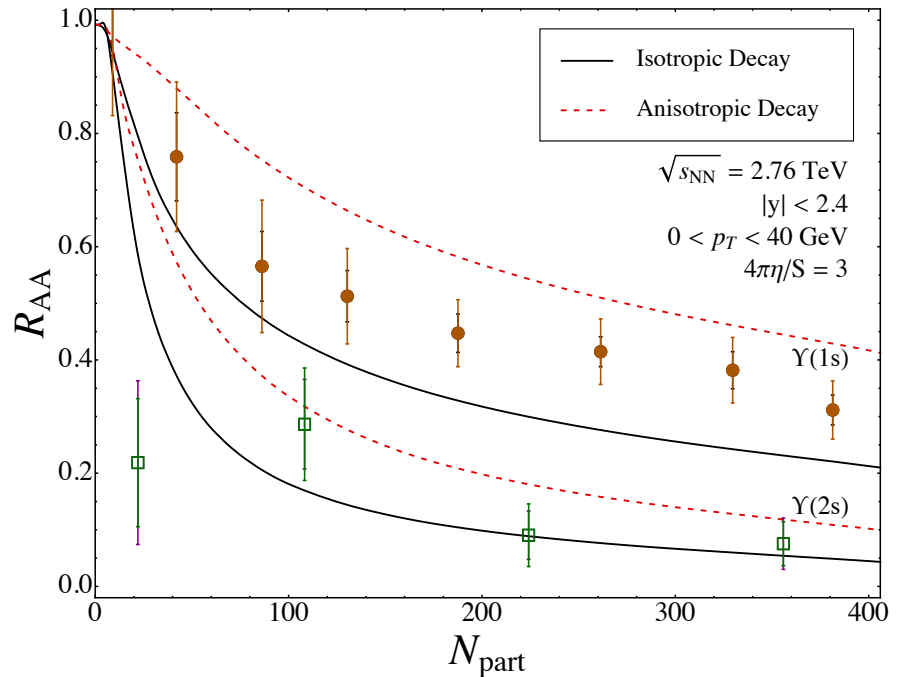
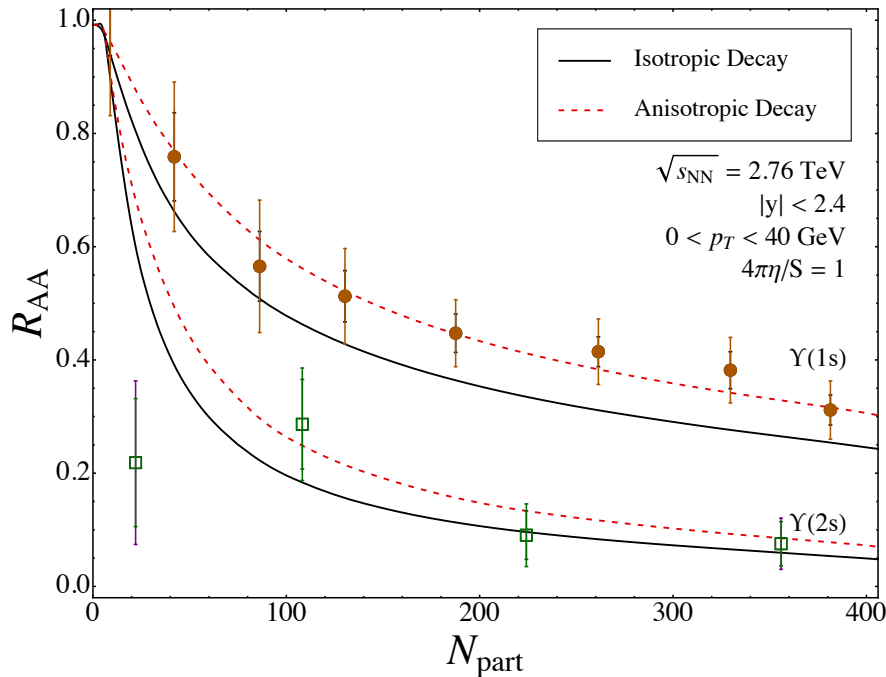
[Laine et al hep-ph/0611300](#)

- Used this as a model for the free energy (F) and also obtained internal energy (U) from this.

$$V_{\text{I}}(\mathbf{r}) = -C_F \alpha_s p_{\text{hard}} \left[\phi(\hat{r}) - \xi (\psi_1(\hat{r}, \theta) + \psi_2(\hat{r}, \theta)) \right]$$

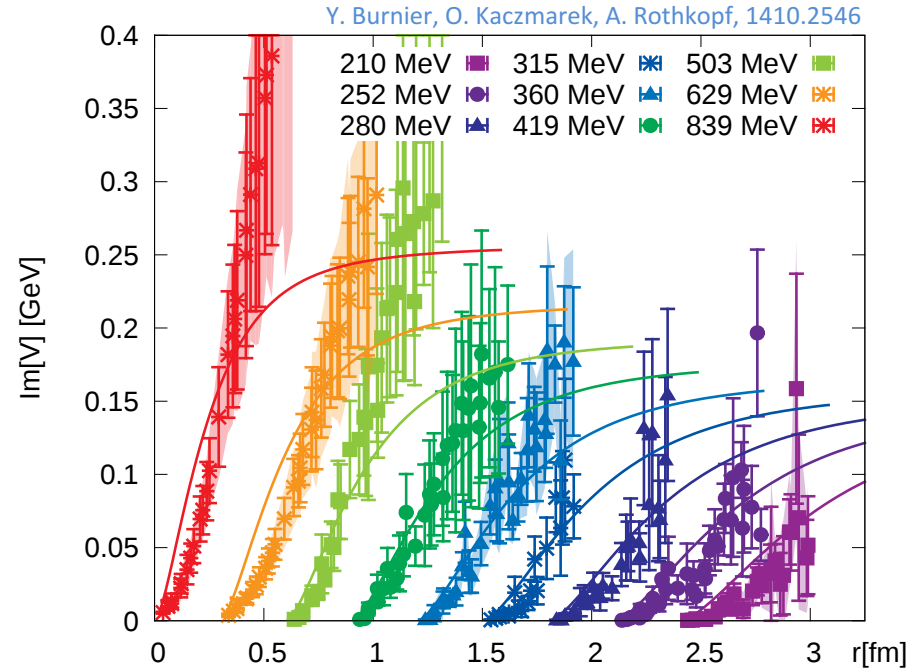
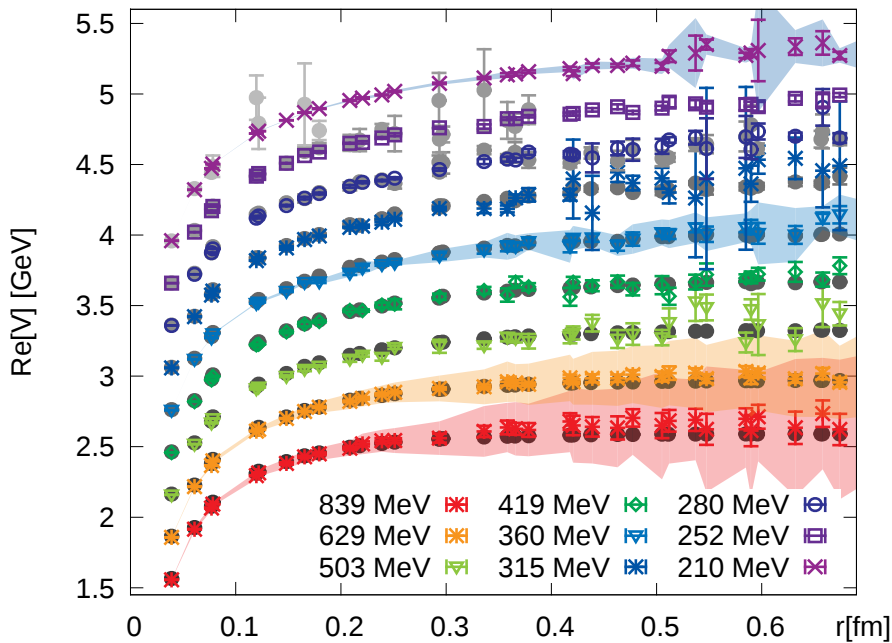
[Dumitru, Guo, and MS, 0711.4722 and 0903.4703](#)
[Burnier, Laine, Vepsalainen, arXiv:0903.3467 \(aniso\)](#)

Anisotropy effect @ 2.76 TeV



- Including the anisotropy effect in the potential etc is important
- The two figures above show what happens if we simply use the isotropic potential with the local effective temperature determined from the energy density

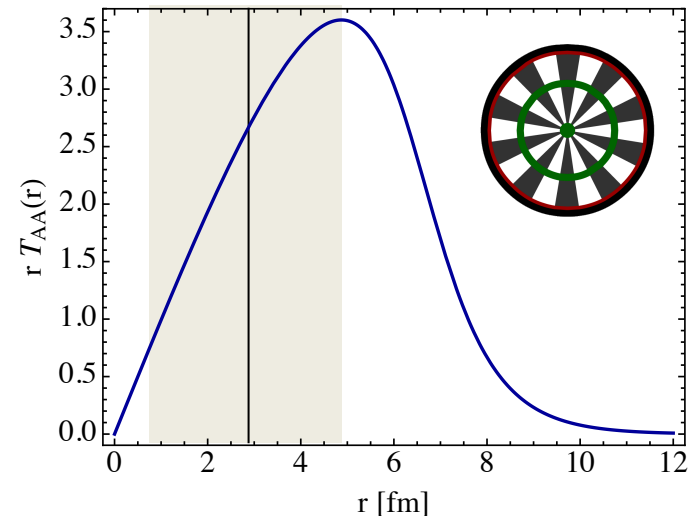
Sanity check



- Results above are the real and imaginary part of the heavy quark potential extracted from the lattice.
- For the imaginary part, the authors also compare with the isotropic $\text{Im}[V]$ indicated on the previous slide.

Good news and bad news

- Large binding energies \rightarrow short formation times
- Formation time for $Y(1s)$, for example, is ≈ 0.2 fm/c
- This comes at a cost: **We need to reliably model the early-time dynamics since quarkonia are born into it.**
- In addition, production vertices can be anywhere in the transverse plane, not just the central hottest region.
- For example, for a central collision $\langle r \rangle \sim 3.2$ fm and the most probable r is ~ 5 fm.
- **We need to reliably describe the dynamics in the full 3+1d volume.**



The suppression factor

- Resulting decay rate $\Gamma_T = -2 \text{Im}[E_{\text{bind}}]$ is a function of τ , \mathbf{x}_\perp , and ς (spatial rapidity). First we need to integrate over proper time

$$\bar{\gamma}(\mathbf{x}_\perp, p_T, \varsigma, b) \equiv \int_{\max(\tau_{\text{form}}(p_T), \tau_0)}^{\tau_f} d\tau \Gamma_T(\tau, \mathbf{x}_\perp, \varsigma, b)$$

- From this we can extract R_{AA}

$$R_{AA}(\mathbf{x}_\perp, p_T, \varsigma, b) = \exp(-\bar{\gamma}(\mathbf{x}_\perp, p_T, \varsigma, b))$$

- Use the overlap density as the probability distribution function for quarkonium production vertices and geometrically average

$$\langle R_{AA}(p_T, \varsigma, b) \rangle \equiv \frac{\int_{\mathbf{x}_\perp} d\mathbf{x}_\perp T_{AA}(\mathbf{x}_\perp) R_{AA}(\mathbf{x}_\perp, p_T, \varsigma, b)}{\int_{\mathbf{x}_\perp} d\mathbf{x}_\perp T_{AA}(\mathbf{x}_\perp)}$$